Contrasting effects of environment and genetics generate a continuum of parallel evolution

Yoel E. Stuart[1]*, Thor Veen[1†], Jesse N. Weber[1†], Dieta Hanson[2], Mark Ravinet[3], Brian K. Lohman[1], Cole J. Thompson[1], Tania Tasneem[4], Andrew Doggett[4], Rebecca Izen[1], Newaz Ahmed[1], Rowan D. H. Barrett[2], Andrew P. Hendry[2], Catherine L. Peichel[5†] and Daniel I. Bolnick[1]

Parallel evolution of similar traits by independent populations in similar environments is considered strong evidence for adaptation by natural selection. Often, however, replicate populations in similar environments do not all evolve in the same way, thus deviating from any single, predominant outcome of evolution. This variation might arise from non-adaptive, population-specific effects of genetic drift, gene flow or limited genetic variation. Alternatively, these deviations from parallel evolution might also reflect predictable adaptation to cryptic environmental heterogeneity within discrete habitat categories. Here, we show that deviations from parallel evolution are the consequence of environmental variation within habitats combined with variation in gene flow. Threespine stickleback (*Gasterosteus aculeatus*) in adjoining lake and stream habitats (a lake–stream 'pair') diverge phenotypically, yet the direction and magnitude of this divergence is not always fully parallel among 16 replicate pairs. We found that the multivariate direction of lake–stream morphological divergence was less parallel between pairs whose environmental differences were less parallel. Thus, environmental heterogeneity among lake–stream pairs contributes to deviations from parallel evolution. Additionally, likely genomic targets of selection were more parallel between environmentally more similar pairs. In contrast, variation in the magnitude of lake–stream divergence (independent of direction) was better explained by differences in lake–stream gene flow; pairs with greater lake–stream gene flow were less morphologically diverged. Thus, both adaptive and non-adaptive processes work concurrently to generate a continuum of parallel evolution across lake–stream stickleback population pairs.

Parallel evolution occurs when phenotypes evolve in the same way in replicate populations adapting to similar habitats[1,2] and is strong evidence for the importance of natural selection in adaptive evolution[2–7]. As an exemplar, marine Threespine stickleback (*Gasterosteus aculeatus*) have independently colonized many freshwater habitats[8–12] in which they repeatedly evolved reduced armour[1], probably in response to differences in predator regimes and salinity. However, even such iconic examples of parallel evolution often present many exceptions[13–16]; that is, replicate populations vary in the magnitude or even in the direction of trait evolution (for example, for stickleback armour, see refs [16–19]).

Deviations from parallel evolutionary responses to similar habitats are frequently attributed to non-adaptive, population-specific conditions[20], such as insufficient genetic variation[19], gene flow between habitat types[21], genetic drift[22] or population age[23]. In such cases, the extent of phenotypic parallelism should covary with population genetic measures that mirror these processes. Alternatively, or additionally, deviations from parallelism might reflect adaptive responses to quantitative environmental differences among qualitatively similar habitats (for examples, see refs [3,13]). In the case of adaptive responses to environmental differences, the extent of phenotypic parallelism should covary with measures of environmental heterogeneity. To date, however, it remains unusual for studies to make quantitative (rather than only qualitative) assessments of whether patterns of parallel evolution

result from non-adaptive processes or from adaptive responses to environmental heterogeneity among seemingly replicate habitats (see refs [24–27] for exceptions). As a result, the processes shaping deviations from parallelism remain poorly understood. Here, we analyze multivariate phenotypic, environmental and genetic variation among 16 replicate lake-and-adjoining-stream population sets of Threespine stickleback (hereafter, lake–stream pairs). This replication allows us to test whether deviations from parallel phenotypic (or genomic) evolution are attributable to non-adaptive population genetic phenomena, adaptive responses to environmental heterogeneity, or both.

Results and discussion

In many watersheds on Vancouver Island, British Columbia, stickleback colonized lake and stream habitats following the Last Glacial Maximum. Despite very close geographical proximity of lake and stream sites, pairs often show strong morphological and genetic lake–stream divergence[13,14,28], probably due to differences in abiotic (for example, flow and depth) and biotic (for example, predator, prey and parasite) parameters between habitats. Critically, previous studies of lake–stream phenotypic divergence in a few focal traits from a few lake–stream pairs have shown that there is some strikingly parallel lake–stream divergence, but that there is also considerable variation among pairs and traits in the magnitude and direction of divergence[13,14]. We used this variation to infer and compare the

processes shaping evolution by first quantifying the extent of phenotypic parallelism among 16 lake–stream pairs, each from a different watershed (Supplementary Table 1 and Supplementary Fig. 1). At least 11 of these pairs represent independent evolutionary replicates of lake–stream divergence as inferred from genetic analysis showing adjacent pairs as sister populations (Supplementary Fig. 1).

We documented a continuum of phenotypic parallelism in 86 phenotypic traits (see Methods) that describe various aspects of body shape, defensive armour, swimming ability and trophic morphology (Supplementary Table 2). In a trait-by-trait linear modelling approach, we found that 72% of traits showed a significant main effect of habitat, indicating that lake–stream trait differences are to some degree consistent (parallel) across replicate pairs (Fig. 1). In some cases (above the 1:1 line in Fig. 1a) the effect was relatively large; for instance, lake stickleback had more gill rakers than their stream neighbours in 14 out of 16 pairs (Fig. 1b), a result consistent with previous studies[13,14]. However, the direction or magnitude of the habitat effect differed among pairs for every trait (significant habitat × pair interaction effects; for example, Fig. 1c–e). Thus, lake–stream divergence for a particular trait ranged from highly parallel to non-parallel to antiparallel, with various pairs falling into different places on this continuum of parallel evolution depending on the trait. In short, populations in ostensibly similar environments vary appreciably in their extent of parallel phenotypic lake–stream divergence, and this variation differs among traits. Indeed, for most traits, the habitat-by-pair interaction is stronger than the main effect of habitat (Fig. 1, below the 1:1 line), indicating that deviations from parallel evolution are typical.

To formally quantify this variation in phenotypic divergence in multivariate trait space, we used a vector analysis approach pioneered by Adams and Collyer[29]. Lake–stream divergence within each pair can be described by a vector connecting the multivariate phenotypic mean (centroid) of fish in a lake to the multivariate phenotypic mean of fish in the adjoining stream (Fig. 2). Phenotypic vector length (L_P) then represents the magnitude of lake–stream morphological divergence for each lake–stream pair, whereas the vector direction through trait space measures the relative weight of different traits in contributing to lake–stream divergence (Fig. 2). Strict parallel evolution exists when two such divergence vectors (for instance, lake to stream in pair i and lake to stream in pair j) have the same direction (the angle between the two vectors $\theta_{P,\{i,j\}} \approx 0°$) and the same magnitude ($\Delta L_{P,\{i,j\}} = L_{Pi} - L_{Pj} \approx 0$). Deviations from parallelism are revealed by significant non-zero angles between vectors ($\theta_P > 0°$) or significantly different vector lengths ($\Delta L_P \neq 0$). This vector approach thus effectively reduces a massively multivariate dataset to several summary statistics, which provide a formal quantification of parallelism. This quantitative approach allows us to test whether environmental or demographic variables covary with the extent of parallel evolution.

Multivariate vector analysis on 84 phenotypic traits (see Supplementary Information and Supplementary Table 2) confirmed a continuum of parallelism with more parallel lake–stream divergence between some pairs and less between others (Fig. 3a), matching the trait-by-trait result that highly parallel divergence is rare (Fig. 1). Note that Fig. 3a uses a principal component analysis to focus on two axes, for the sake of visual depiction, whereas statistical analyses (reported hereafter) were based on a higher-dimensional analysis of all 84 traits (Fig. 3b,c), for which evolution was less parallel. The smallest and largest multivariate angles between any two lake–stream vectors were 30° and 135°, respectively (Fig. 3b), and nearly all angles were significantly different from zero (Supplementary Table 3). Comparing lake–stream divergence vectors pairwise across all possible lake–stream pairs, the average angle θ_P (± s.d.) between vectors was $81.1 \pm 26.4°$ (Fig. 3b); that is, phenotypic vectors were nearly orthogonal to one another on average, although variation in parallel divergence ranged from highly parallel pairs to non-parallel
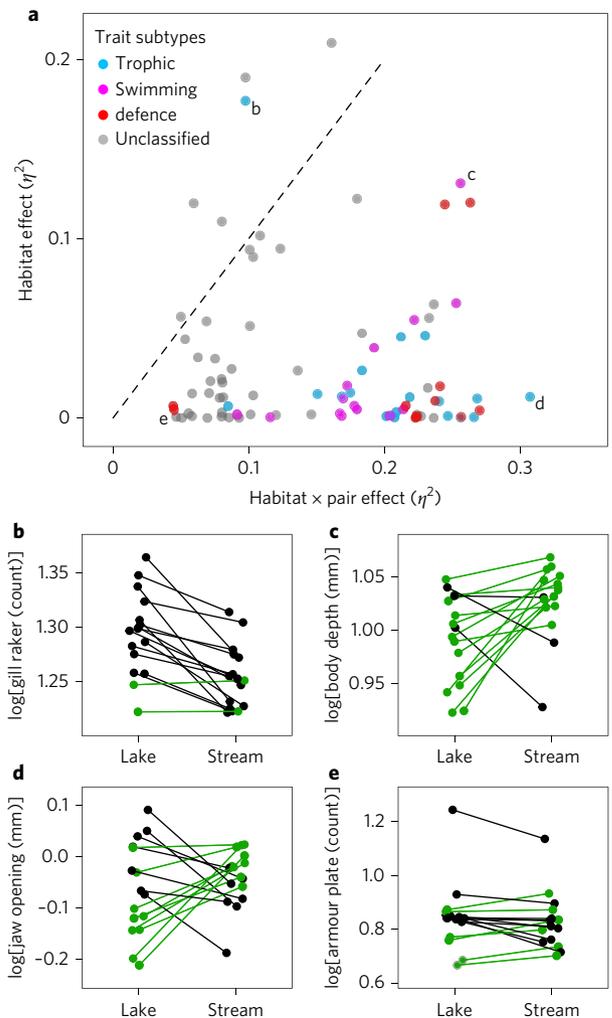

Figure 1 | Variation in the extent of parallel evolution among individual phenotypic traits, each tested separately. a, For each trait (Supplementary Table 2), we used a linear model to estimate the effect size (Eta^2 = η^2) for the effects of habitat (lake versus stream), pair and the habitat × pair interaction on variation in the focal trait. Habitat η^2 indicates the extent to which any given trait diverges predictably from lake to stream (that is, in parallel). The η^2 for the habitat × pair interaction measures the extent to which lake–stream phenotypic divergence varies across pairs (that is, deviates from parallel); every trait showed a significant habitat × pair effect. η^2 for the effect of pair itself is not plotted here. The dashed line is a 1:1 line, for ease of visualization; points falling above this line have a larger habitat effect than interaction effect (that is, parallel exceeds non-parallel divergence) and vice versa. We plot effect sizes for each of 86 phenotypic traits (points) to illustrate the overall trend towards deviation from parallel evolution (that is, relatively larger interaction than habitat effects). Some traits are colour-coded by *a priori*-designated functional subgroups; grey points are geometric morphometric coordinates or linear traits that were not *a priori* assigned to a subgroup (Supplementary Table 2). **b–e**, To illustrate non-parallel divergence for individual traits, we plot representative traits from different areas of η^2-space (**b–e** correspond to points b–e in the main panel). Each subplot shows mean trait value (jittered) for each lake and each stream. Each pair's lake and stream are connected by a line, which is colour coded green or black to indicate the increase or decrease, respectively, in trait value from lake to stream. Panel **a** shows a case where trait evolution is highly parallel: 14 of 16 pairs have more gill rakers in lake versus stream. Panel **c** shows a case where lake–stream divergence deviates from parallel: 7 of 16 pairs have longer opening inlevers in lake populations. Traits are log transformed and size corrected.
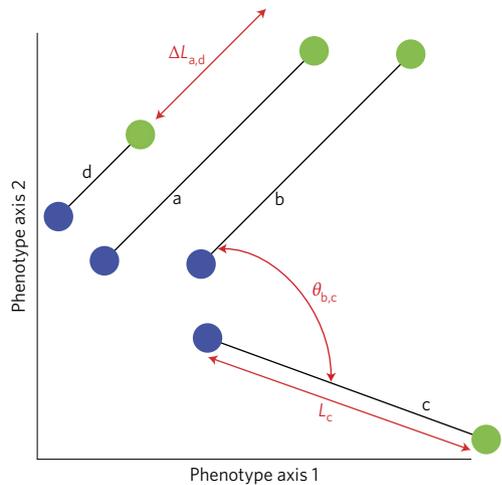
Figure 2 | Calculation of L, ΔL and θ. Hypothetical lake–stream phenotypic divergence vectors for four lake–stream pairs: a, b, c and d. Lake means (blue) and stream means (green) are plotted, and the black line connecting each pair is the divergence vector. Three statistics are shown in red. L_c is the length of divergence vector c. L can be calculated for every lake–stream pair. ΔL_P is the difference between the lengths of any two vectors (for example, $L_a - L_d$). $\theta_{b,c}$ is the angle between divergence vectors b and c and represents the difference in direction of lake–stream divergence between any two pairs. A difference in direction indicates that different phenotypic traits contribute to each pair's lake–stream divergence. Both ΔL and θ can be calculated between any two pairs of lake–stream populations, generating distance matrices for both statistics. We plot two-dimensional vectors for ease of interpretation, but we use multidimensional vectors in our analyses (for example, our phenotypic vector analysis relies on 84 traits).
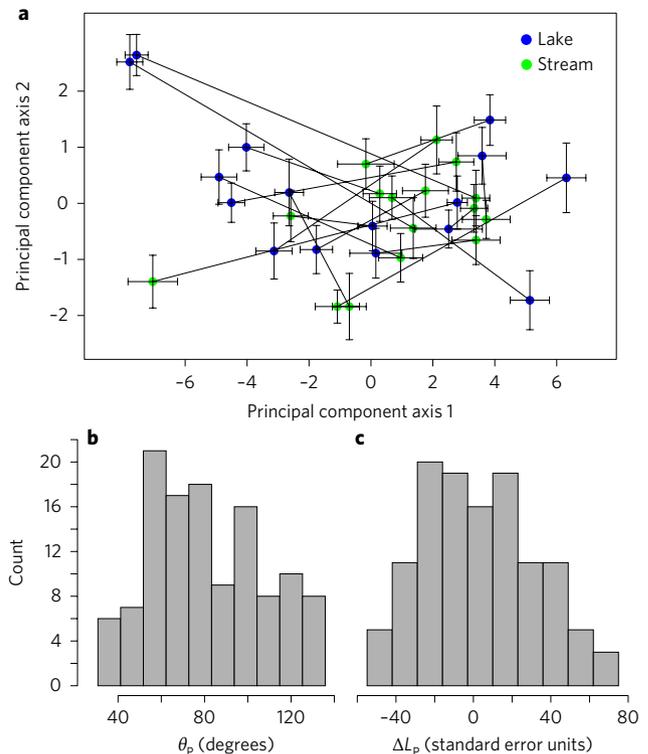

Figure 3 | Replicate lake–stream pairs exhibit variation in extent of parallel divergence. a, The phenotypic means (centroids) for each of 16 lake populations of stickleback (blue dots) are connected by lines to their parapatric stream population means (green dots) and plotted for the first two principal component axes in morphospace (with standard error bars; $n \approx 40$ fish per population; Supplementary Table 1). Principal component 1 (35% of variance) loads weakly and fairly evenly on standard length, geometric morphometric centroid size and most of our size-corrected linear trait measures. Principal component 2 (12% of the variance) loads weakly though fairly evenly on the generalized procrustes analysis-transformed body shape coordinates. **b**, Histogram of the 120 (pairwise) angles between lake–stream phenotypic divergence vectors (θ_P) in degrees. **c**, Histogram of the 120 differences in length between phenotypic divergence vectors (ΔL_P). These histogram values are based on the multivariate vectors from the entire 84-trait morphological dataset (not the principal component axes visualized in **a**).

pairs to anti-parallel pairs (most vector angles differed significantly from 90°; Supplementary Table 3). The differences in phenotypic vector lengths were similarly variable, with a mean ΔL_P ($\pm$ s.d.) of 3.7 ± 29.4 standard error units (Fig. 3c and Supplementary Table 3). In short, pairs vary greatly in their directions and magnitudes of lake–stream divergence. We next aimed to explain this variation among the pairs along the parallelism continuum.

We hypothesized that such variation in phenotypic lake–stream divergence among pairs partly reflects adaptation to quantitative environmental variation not captured by the binary lake-versus-stream categorization. To test this hypothesis, we used the same vector analysis approach, as described in the Methods, to summarize multivariate lake–stream differences in environmental characteristics (for example, depth, flow and vegetation structure; see Supplementary Table 4 for a full list of environmental variables) in terms of lengths (L_E), length differences (ΔL_E) and angles (θ_E) among environmental vectors. Similar to our phenotypic results, lake–stream parallelism in multivariate environmental space also varied depending on which environmental traits and replicate pairs were being compared (Supplementary Figs 2 and 3; mean θ_E ($\pm$ s.d.) = $85.4 \pm 11.7°$; mean ΔL_E ($\pm$ s.d.) = 0.41 ± 4.3 standard deviation units). Consistent with our hypothesis, this quantitative representation of environmental heterogeneity explained variation in phenotypic parallelism among pairs. Specifically, the angles between phenotypic vectors (θ_P) were positively correlated with the angles between environmental vectors (θ_E) across the 16 pairs (Mantel test: Pearson's product moment correlation coefficient (r) = 0.29; $P = 0.01$; Fig. 4a). From these trait–environment correlations, we infer that deviations from parallel phenotypic evolution in this system are at least partly adaptive.

Unlike the vector directions (θ_P and θ_E), however, the magnitudes of environmental and phenotypic vectors were not correlated

(L_P versus L_E linear model: adjusted coefficient of determination (R^2) = −0.07, $P = 0.83$; ΔL_P versus ΔL_E Mantel test: $r = -0.07$, $P = 0.78$; Fig. 4c,e). Given that increasingly divergent habitats are expected to favour increasingly divergent phenotypes, this non-correlation implies the action of some constraint on divergence, which might arise from within-pair lake–stream gene flow[30]. We tested this prediction by quantifying the correlation between phenotypic divergence vectors and genetic divergence vectors. For genetic divergence vectors, we used double digest restriction associated DNA sequencing (ddRADseq)[31] to obtain 78,224 single nucleotide polymorphisms (SNPs) spanning the genome that were variable in at least one population (see Methods). To obtain a set of markers likely to reflect neutral population genetic processes (as opposed to selection), we then excluded the top 5% of lake-versus-stream F_{ST} outliers within each pair, yielding 67,123 SNPs with a mean of 21,544 SNPs per pair (s.d. = 8,904). Of these markers, the average number of SNPs shared across pairs was 10,601 (range: 1,695–23,924). We then ran principal component analysis on this non-outlier SNP set and calculated lake–stream divergence vectors in genetic principal component space to compute θ_G, L_G and ΔL_G. We found that the magnitude of non-outlier, genetic lake–stream divergence was positively
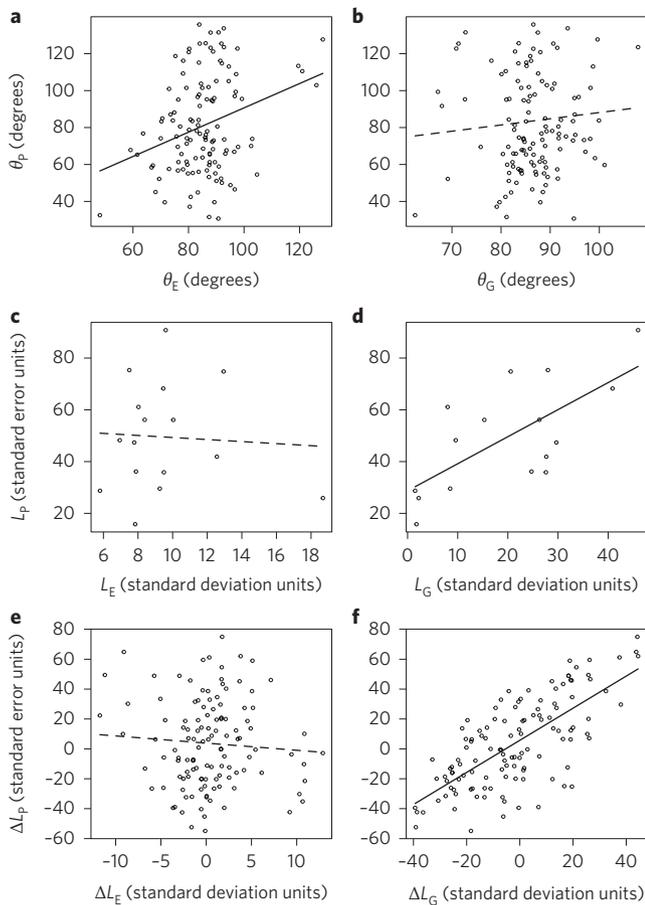
Figure 4 | Comparisons among 16 pairs reveal that deviations from parallel phenotypic divergence are correlated with both environmental (first column) and genetic (second column) deviations from parallel.
a, Pairwise angles between phenotypic vectors (θ_P) plotted against corresponding angles between environmental vectors (θ_E). The significant trend is robust to excluding the four points in the top right, which are not outliers in other regards. **b**, Angles between phenotypic vectors (θ_P) are plotted against angles between genomic vectors (θ_G). **c,d**, Phenotypic divergence vector lengths (L_P) for each lake–stream pair plotted against corresponding environmental (L_E) and genomic (L_G) vector lengths, respectively. **e,f**, Differences in magnitude between phenotypic vectors (ΔL_P) plotted against corresponding differences in magnitude between environmental (ΔL_E) and genomic (ΔL_G) vector lengths, respectively. Relationships for θ, L and ΔL are visualized by regression lines, whose significance (solid = significant) is determined by Mantel tests (for θ and ΔL) or linear regression (for L).

correlated with the magnitude of phenotypic lake–stream divergence (L_G versus L_P linear model: adjusted $R^2 = 0.44$, $P = 0.003$; ΔL_G versus ΔL_P Mantel test: $r = 0.71$, $P = 0.001$; Fig. 4d,f). We interpret this positive association as an indication that homogenizing gene flow constrains adaptive divergence.

To strengthen this last inference, we used approximate Bayesian computation (ABC) to estimate the time since lake–stream divergence and the number of lake–stream migrants per generation (Nm) for each of the 16 pairs (Supplementary Information). As an external validation of these estimates, the ABC migration rate estimates were significantly negatively correlated with the physical distance between lake and stream sample sites. Using multiple regression, the magnitude of phenotypic divergence, L_P, decreased significantly as a function of the estimated gene flow (Nm), while showing a weak but non-significant tendency to increase with

divergence time (Supplementary Table 5; full model adjusted $R^2 = 0.51$, $F_{2,13} = 8.8$, $P = 0.004$; Nm: $t = -3.7$, $P = 0.003$, Supplementary Fig. 4; divergence time: $t = 1.6$, $P = 0.12$). We interpret these associations and analyses as consistent with the expectation[30] that gene flow constrains adaptive divergence. The opposite causal pathway is also theoretically possible; that is, adaptive divergence to different habitats (that is, large L_E) might induce reproductive isolation and inhibit gene flow. We consider this alternative 'ecological speciation' scenario[21] to be less likely because it would also predict gene flow to be lower between more environmentally divergent pairs. We found no correlation between L_E and L_G (linear model adjusted $R^2 = -0.07$, $P = 0.82$), suggesting that gene flow is the causal force influencing the magnitude of adaptive divergence in this system.

As expected for neutral loci[21], the direction of non-outlier genetic divergence (mean $\theta_G \pm$ s.d. $= 86.4 \pm 7.2°$) was uncorrelated with both phenotypic (θ_G versus θ_P Mantel test: $r = 0.06$, $P = 0.27$; Fig. 4b) and environmental (θ_G versus θ_E Mantel test: $r = 0.12$, $P = 0.13$) vector directions. However, we expected different outcomes for the outlier loci. In particular, genomic targets of selection should diverge in a manner consistent with both phenotypic and environmental parallelism. We found the SNPs showing outlier lake–stream allele frequency divergence (top 5% F_{ST}, which could at least be linked to selected loci) to be shared between some but not all lake–stream replicates. In particular, lake–stream pairs tended to share more outlier SNPs if they were environmentally or phenotypically more parallel (Mantel tests: $\theta_{OUTLIERS} \approx \theta_E$, $r = 0.22$, $P = 0.05$; $\theta_{OUTLIERS} \approx \theta_P$, $r = 0.19$, $P = 0.07$; Supplementary Fig. 5). Hence, we infer that parallel phenotypic divergence arises in part by parallel evolution of divergently selected loci. This outlier analysis corroborates a recent common garden study[32] on three of the populations included here, which together suggests that much (but not all) of the lake–stream phenotypic divergence we have observed has a genetic basis.

Conclusion

Ostensibly, lake and stream stickleback pairs should be prime candidates for highly parallel evolution. They dwell in discrete and divergent habitats, and they are recently derived from the same ancestral marine population, increasing the likelihood of them reusing similar ancestral genetic variants for adaptation. Nevertheless, we found that the simple lake-versus-stream habitat categorization was too coarse to adequately capture evolutionary responses to quantitative environmental variation. Specifically, our analysis revealed that phenotypic parallelism varies dramatically among traits and population pairs. Variation along this continuum of parallelism, from highly parallel to non-parallel to anti-parallel, is not merely the result of stochastic processes eroding otherwise deterministic evolution. Instead, what might initially appear to be idiosyncratic divergence across apparently similar habitats actually reflects deviations from parallel natural selection—because specific environmental conditions vary among instances of each habitat category. Additional variation in parallelism arises when this 'cryptic' determinism is constrained by variation in lake–stream gene flow among populations. Thus, multivariate, quantitative analysis of continuous variation in environmental, morphological and genetic parallelism shows how multiple evolutionary processes interact simultaneously to shape evolutionary divergence and parallelism in nature.

Methods

Stickleback sampling. In May to July 2013, we collected Threespine stickleback from one lake and its inlet or outlet stream from each of 16 watersheds on Vancouver Island, British Columbia, Canada (32 sites in total; Supplementary Table 1). We also collected stickleback from three marine sites (Supplementary Table 1) to represent the ancestor that likely colonized each of these watersheds[9,12].

We captured fish primarily using 50 unbaited minnow traps set haphazardly across a transect of approximately 100 m to include all available habitat at a site, except for very deep locations that we could not reach; typically, the deepest traps yielded very few stickleback. Sample sizes at several sites were augmented with dip

net capture when fish were trap shy. Though we aimed for three-hour soak times, at some sites, longer soak times or additional trappings were performed to increase sample sizes. We retained the first 80 captured adult fish at each site, and these fish were euthanized with MS-222 buffered with sodium bicarbonate. We clipped the right pectoral fin of each fish and stored it in 100% ethanol for DNA preservation. The specimens were preserved in 10% buffered formalin for at least 14 days, then rinsed, stained with alizarin red, and stored in 40% isopropanol. Approximately 40 fish per site were chosen haphazardly from our collections to measure morphological variation. A sample size of 40 suffices for stickleback, for most quantitative traits, to return a normal distribution. Of those 40, a subset of 24 fish were genotyped. Of those 24, 15 fish were dissected for gut contents to quantify both diet and macroparasite infections.

Morphology. *Specimen photography.* We collected linear measurements and body shape information from each fish using digital landmarks placed on photographs of the left lateral side and of the ventral surface. Photographs were taken under standardized lighting conditions with a ruler for scale. To aid in digital landmark placement, we inserted specimen pins before photography at the base of the skull on the dorsal midline, the anterior and posterior insertions of the dorsal fin and anal fin, the caudal tip of the posterior process of the pelvic girdle, the anterior edge of the pelvic girdle along the midline, the anterior tip of the ectocoracoid, and the insertions of the pectoral fin, following ref. [13]. Dorsal spines were erected. Fish were pinned flat to remove preservation effects. Left pectoral fins were cut from each fish and splayed for the photograph. After external measurements were completed, several additional traits were measured via dissection (for example, gill raker).

Body shape and linear measurements. We used geometric morphometrics to estimate body shape[33]. With tpsDig2 software (Rohlf 2006), we placed 19 landmarks on lateral images of each fish, following ref. [25], except that we included landmarks on the caudal tip of the posterior process of the pelvic plate, on the anterior edge of the anterior process of the pelvic plate on the midline and on the dorsal-most point of the eye; we excluded the 'slider' landmark denoting the posterior edge of the operculum. We used the R package 'geomorph'[34] to extract individual centroid size and to run generalized procrustes analysis (function 'gpagen') to align the landmarks using a generalized least squares superimposition procedure. We retained the new x and y coordinates from each fish for analysis. We treated these coordinates as traits, rather than use relative warps, because performing statistics on only a subset of relative warps ignores valuable data. Using all of the relative warps retains all of the data, but the axes are rotated and less interpretable than just using all coordinates. Using coordinates also allows us to remain agnostic to the relationships among, and importance of, traits. Moreover, individual trait coordinates have been shown to have their own quantitative trait loci[35]. To augment estimates of body shape, univariate measurements were digitized from photographs using the program Fiji[36] with the plugin ObjectJ (https://sils.fnwi.uva.nl/bcb/objectj/), through dissection and with calipers; these measurements are described in Supplementary Table 2.

Environment. *Habitat.* To characterize the environment of each site, we measured habitat variables for at least 50 traps per site, including flow rate, depth, and categorical scores describing the substrate, bank and vegetation (Supplementary Table 4). The remainder of the environmental variables were measured at the levels of site (for example, water quality) and fish (for example, stomach contents and parasite infection status) (Supplementary Table 4).

Stomach contents. Estimates of diet from stomach contents are relatively reliable measures of long-term diet, as revealed by stable isotope analysis[13,37]. We dissected the stomachs of 15 fish from each population and identified the contents to the lowest feasible taxonomic level under a dissecting microscope. These 15 fish were a subsample of the 24 fish we genotyped (described below). Gut contents were identified by a single person (T.T.); a sample size of 15 per population was targeted because that was the maximum number that could be processed during T.T.'s summer hire. Only five fish from each population were dissected at a time, and populations were cycled through until 15 fish had been sampled.

Parasite infection status. In the same 15 fish dissected for stomach contents, T.T. also documented parasite diversity. For two parasites, the cestode *Schistocephalus solidus* and the nematode *Eustrongylides* spp., Y.E.S. dissected nine more fish to complete the set of 24 genotyped fish (see below) to augment other laboratory projects investigating the genetic underpinnings of tolerance and resistance to these two parasites.

Genetics. *DNA extraction.* DNA was extracted in 96-well plates using the Promega Wizard SV Genomic DNA Purification kit. Extractions were quantified fluorometrically to facilitate downstream sequencing steps, using the Life Technologies PicoGreen dsDNA assay on an Infinite M200 Pro plate reader (Tecan).

ddRADseq. To estimate genetic diversity within sites, across the lake–stream boundary and among pairs, we used ddRADseq[31] to generate markers spanning the

genome. We prepared ddRADseq libraries for 24 individual fish per lake and per stream, for each of the 16 pairs, as well as the three marine sites.

Briefly, we used NlaIII and MluCI (New England Biolabs) to digest our genomic samples, as these restriction enzymes were estimated to provide sufficient RAD fragments to type ~50,000 high-quality SNPs, thereby generating dense, genome-wide marker coverage. We pooled 48 individuals into each library after first ligating one of 48 uniquely barcoded P1 flex-adapters[31] to each individual. We gel-extracted fragments 371–416 base pairs (bp) in size using a Pippen Prep 2% MarkerB 100–600 bp cassette (Sage Science). This selection window includes genomic fragments of 295–340 bp and accounts for the 76 bp added with P1 and P2 adapters. Post-size selection, we used streptavidin-coupled beads (Dynabeads M-270, Invitrogen) to isolate fragments possessing at least one biotin-tagged P2 adapter. We then divided libraries into several aliquots, amplified each aliquot by PCR (12 cycles, Phusion High Fidelity PCR kit, New England Biolabs) and pooled those aliquots. We used solid-phase reversible immobilization beads (Sera-mag Speedbeeds, Fisher) to clean samples after each enzymatic step[38]. We finished with a library of 48 individuals for each of the 16 lake–stream pairs. In addition, we generated two 48-individual libraries consisting of three marine populations (24 individuals each) and 24 duplicate fish sampled from the lake–stream pairs. All 18 libraries were pooled at equimolar concentrations and then sequenced across 12 lanes on an Illumina Hi-Seq 2500 at the Genome Sequencing and Analysis Facility at the University of Texas at Austin (UT Austin).

Genotyping pipeline. For each library (split by P2 index read), we concatenated R1 and R2 fastq.gz files from across multiple sequencing runs into single R1 fastq.gz and R2 fastq.gz files using Unix. We then used Stacks[39] version 1.13 (process_ radtags -P, -p, -r, -i, --inline_index, --disable_rad_check) to de-multiplex by individual. For downstream processing, we altered the R1.fa or R2.fa files to make FASTA headers match. Unix code for this step is available from the authors.

We downloaded the stickleback genome (version 078; current as of January 2015) from www.ensembl.org for read mapping, alignment and genotyping of sequences. We initially mapped sequences to this genome build using the Burrows–Wheeler Aligner software package[40] (version 0.7.7-r441) and performed secondary alignments using Stampy[41] (version 1.0.23). We used SAMtools[42] (version 0.1.19-44428cd) to convert the resulting .sam file to .bam format for genotyping. A Unix shell script containing SAMtools and Stampy commands is available from the authors.

The large number and sizes of our .bam files made it computationally intractable to simultaneously consider all individuals and genomic positions when calculating genotype probabilities. We therefore took a two-step approach that allowed us to partition the genome into only those sites that were variable in at least one pair and then compare this subset of positions among all pairs. First, we calculated genotype probabilities for sites (excluding indels) in each pair separately using the 'mpileup' algorithm in SAMtools (options: -C 50, -E, -S, -D, -u, -I). Then, we created genotype files using the SAMtools function 'BCFtools view' (options: -v, -c, -g), keeping only variant sites. We generated a .bed file containing a list of all sites that were polymorphic somewhere in the 16 pairs and again used mpileup (options: flags -C 50, -E, -S, -D, -u, -I, -l where -l specified the .bed file) to calculate genotype probabilities at every one of these positions from our .bam files. This second mpileup command was run on six pools of individuals. Each pool comprised four individuals from each collection locality. We then used BCFtools again (using view -v, -c, -g) to call bi-allelic SNPs on every individual.

Filtering was performed by depth and completeness. We used VCFtools (version 0.1.12b; http://vcftools.sourceforge.net/index.html) for all filtering steps. After examining variation in mean read depth per site across all individuals, as an initial filter we chose to retain sites that were sampled relatively frequently, but not often enough to suggest paralogous mapping. We removed all sites with a mean depth of less than 1 or greater than 75 (commands: --min-meanDP and --max-meanDP). We then filtered by minimum and maximum read coverage per site within individuals (commands: --minDP and --maxDP) set to 8 and 100, respectively. Finally, we filtered by among individual completeness (command: --max-missing), keeping only sites present in at least 80% of individuals. We output the final filtered dataset using VCFtools --012, which creates a matrix with individual fish as rows, SNP positions as columns and data entered as 0, 1 or 2, representing the number of non-reference alleles.

Analysis. We visually inspected the data for outliers and strong deviations from normality, which would require non-parametric statistical approaches. Every trait, except left and right side plate numbers, was unimodally distributed and approximately normal. Furthermore, we found no cause to exclude samples or populations from any of our analyses.

Morphological trait size correction. We size corrected 45 linear traits using the following formula: $M_{s,i} = M_{0,i} \times (L_s/L_{0,i})^b$, where $M_{s,i}$ is the size-corrected trait value for individual i, $M_{0,i}$ is the non-size-corrected trait value for individual i, L_s is the overall mean for our log-transformed size-related variable across all individuals, and $L_{0,i}$ is the log-transformed size-related variable of individual i, standard length in this case, for our univariate traits. b is the common within-group slope calculated from a linear mixed model of $\log_{10}(M_{0,i})$ regressed on $\log_{10}(L_{0,i})$, with pair included as a random factor[32,43]. The 45 traits we size corrected were those listed in

Supplementary Table 2, except for standard length and mass. We then combined these size-corrected univariate traits, as well as $\log_{10}$-transformed standard length and mass, with centroid size and our 38 x and y coordinates from our 19 geometric morphometric landmarks, for a total of 86 phenotypic traits.

Trait-by-trait linear models. Trait-by-trait (see Supplementary Table 2 for details), pooling lake and stream individuals (but excluding marine fish), we ran a linear model, trait ~ habitat + pair + habitat × pair, on our phenotypic traits to test for parallel (significant habitat effect) and non-parallel (significant habitat × pair interaction) phenotypic divergence. For each trait's linear model output, we used the EtaSq function (R: BaylorEdPsych) to extract the effect sizes for each term in the model.

Vector analysis. Our multivariate analysis of parallelism centred on the calculation of vectors of three different types of divergence between lakes and streams: morphological, environmental and genetic. Vectors represent the direction and magnitude of divergence between any lake centroid and its stream centroid for each data type. We calculated the angle, θ, between vectors of any two pairs; the length of each divergence vector (L); and the difference in vector lengths between any two pairs (ΔL). θ and ΔL provide intuitive and mathematically formal measures of parallelism (Fig. 2).

To calculate the multivariate (that is, multi-trait) lake–stream phenotypic divergence vector for each lake–stream pair, we ran t-tests comparing the distribution of each trait in a lake to that in its adjoining stream; this had the added benefit of correcting for scale differences among traits, resulting in standard error units. We used every trait from the trait-by-trait analysis except for two (see Supplementary Table 2 for details), totalling 84 traits. Giving equal weight (by using the t-statistic) to each variable allowed us to be agnostic about which traits are important in lake–stream divergence. That is, to use the Boot lake–stream pair as an example, we calculated the lake-versus-stream t-statistic for each of our 84 traits, taking each t-statistic to be an estimate of lake–stream divergence for that trait in the Boot system. Concatenating all 84 t-statistics generated a divergence vector through 84-dimensional morphospace for the Boot lake–stream pair. Building such vectors for all 16 pairs generated a data frame with lake–stream pair on the rows and lake–stream t-statistics for each trait in columns. Thus, each row represented the multidimensional phenotypic lake–stream divergence vector for a given pair (Supplementary Dataset). With these divergence vectors, we calculated the angle between them for every pairwise lake–stream pair comparison, hereafter, θ_P, (P is for phenotype). Angles were calculated by taking the dot product of each pair of divergence vectors, which was the arc-cosine of the Pearson correlation for each vector pair. L_P was the multivariate Euclidean length spanned by each vector. Then, pairwise, we calculated the difference in length between pairs (ΔL_P). Thus, we finished with a 16 × 16 distance matrix of θ_P values, 16 L_P values and a 16 × 16 distance matrix of ΔL_P values.

Environment. The environmental dataset was collected at three different levels: site, trap and fish (see previous text, and Supplementary Table 4). For trap data, continuous variables were scaled by z-transformation. For each categorical variable, we generated a presence–absence matrix with many columns as there were levels of that variable, and scored a 1 if that level was present at that type and a 0 otherwise. Then we ran a principal component analysis (R: prcomp scale = T) on that presence/absence matrix, keeping the principal component scores from a minimum of three principal component axes, or enough axes to explain greater than 67% of the variance. For fish data, parasite infections and stomach content data were transformed to a presence–absence matrix. Pooling all individuals, we z-transformed the presence–absence matrix by each variable. For site data, each variable was z-transformed. Combining all trap, fish and site environmental variables, now standardized to s.d. units (through principal component analysis or z-transformation), we calculated the mean for each site, and then calculated the lake–stream difference for each trait for each pair: our multivariate environmental lake–stream divergence vector. As with morphology, we used these pair vectors to calculate θ_E, L_E and ΔL_E values.

Genetics. The SNPs obtained via ddRADseq[31] were used to estimate population genetic parameters relevant to the role of neutral and adaptive processes in generating deviations from parallel evolution. These analyses include:

1. Pairwise genetic distances among populations. We calculated pairwise Weir–Cockerham unbiased F_{ST}, a measure of population differentiation due to genetic structuring, between each pair of populations for each SNP. We then averaged across all SNPs to obtain a genome-wide measure of among-population divergence. To expand our geographic sampling, we calculated pairwise genetic distances among an expanded dataset of 68 populations. This included the 16 lakes and 16 streams and three marine populations discussed in this paper (24 fish per population) and added an additional 33 populations from Vancouver Island (12 fish per population) that were genotyped with an identical ddRAD-seq protocol. These populations were added to improve our tree, as more taxa generally serve to improve inference of phylogenetic trees. We used the pairwise genome-wide F_{ST} values to construct a neighbour-joining phylogenetic tree for all 68 populations (Supplementary Fig. 1).

2. Parallelism of replicate divergence vectors. We used principal component analysis (R: prcomp) to reduce the large SNP dataset into a smaller number of

quantitative axes of genetic differentiation. Missing data were conservatively imputed using the dataset-wide mean allele frequency for the affected SNP. We saved individuals' scores on the first 45 principal component axes, which cumulatively explained 50% of the SNP genetic variance. We calculated the centroid for each lake and each stream, for these 45 genetic axes, to obtain vectors in genotypic space. Genetic parallelism was measured using vector analysis, as with phenotypic and environmental data, to obtain measures of θ_G, L_G and ΔL_G. We calculated these genetic divergence vectors, and angles between vectors, for two separate subsets of the SNP dataset: SNPs that were non-F_{ST} outliers in all lake–stream pairs (θ_G and ΔL_G) and SNPs that were F_{ST} outliers in at least one lake–stream pair ($\theta_{OUTLIERS}$, $L_{OUTLIERS}$ and $\Delta L_{OUTLIERS}$).

3. Sharing of putatively adaptive loci. For each of our 16 lake–stream pairs, we identified SNPs whose lake–stream F_{ST} fell within the top 5% of estimated values for that pair. These 'outlier SNPs' represent putative targets of lake–stream divergent natural selection. We categorized every SNP as either being an outlier or non-outlier. Next, we considered every pairwise combination of lake–stream pairs and used a Fisher's exact test to evaluate whether they shared more outlier SNPs than expected by chance. We quantified the extent of shared outlier F_{ST} values by calculating a correlation coefficient, across all loci, between every SNP's outlier status (1/0) in the two lake–stream pairs being compared.

Matrix correlations. To test whether variation in parallelism in environment and genetics might correlate with variation in parallelism in morphology, we used Mantel matrix correlations. We used mantel.rtest (R package ade4) with 9,999 permutations to make the following comparisons: θ_P versus θ_E, θ_P versus θ_G, and θ_G versus θ_E; ΔL_P versus ΔL_E, ΔL_P versus ΔL_G, and ΔL_E versus ΔL_G. Relationships between vector lengths (L_P versus L_E, L_P versus L_G, and L_E versus L_G, as well as L_P versus Nm and divergence time; see Supplementary Information for a more in-depth description of our approximate Bayesian computations) were tested using linear regression models. Cook's distance was used to check the leverage of outliers.

Sexes were pooled for all analyses and the results of this pooled analysis are reported here. We also ran analyses separately for each sex, finding similar results and effect sizes.

Data availability. The R code and morphological, genetic and environmental data used in the analyses for this paper are permanently archived on the UT Austin Corral server and can be lassoed at http://web.corral.tacc.utexas.edu/Stuart_2017_NatureEE_Data_Code/. We will provide the data in two batches: (1) immediately, the high level, curated datasets necessary for recreating the analyses and results presented in the paper; and (2) within a year, the raw data, to the extent that we can, including digital images and raw sequence data. We provide both batches of data to meet data-sharing goals of reproducibility and long-term public availability. As we are actively researching these datasets, we kindly ask that researchers contact us if they are planning to use the data for reasons other than reproducing the findings of our paper.

References

1. Colosimo, P. F. *et al.* Widespread parallel evolution in sticklebacks by repeated fixation of ectodysplasin alleles. *Science* **307,** 1928–1933 (2005).
2. Losos, J. B., Jackman, T. R., Larson, A., de Queiroz, K. & Rodriguez Schettino, L. Contingency and determinism in replicated adaptive radiations of island lizards. *Science* **279,** 2115–2118 (1998).
3. Langerhans, R. B. & DeWitt, T. J. Shared and unique features of evolutionary diversification. *Am. Nat.* **164,** 335–349 (2004).
4. Nosil, P., Crespi, B. J. & Sandoval, C. P. Host-plant adaptation drives the parallel evolution of reproductive isolation. *Nature* **417,** 440–443 (2002).
5. Roda, F. *et al.* Genomic evidence for the parallel evolution of coastal forms in the *Senecio lautus* complex. *Mol. Ecol.* **22,** 2941–2952 (2013).
6. Schluter, D., Clifford, E. A., Nemethy, M. & McKinnon, J. S. Parallel evolution and inheritance of quantitative traits. *Am. Nat.* **163,** 809–822 (2004).
7. Huss, M., Howeth, J. G., Osterman, J. I. & Post, D. M. Intraspecific phenotypic variation among alewife populations drives parallel phenotypic shifts in bluegill. *Proc. Biol. Sci.* **281,** 20140275 (2014).
8. McPhail, J. D. Ecology and evolution of sympatric sticklebacks (*Gasterosteus*): origin of the species pairs. *Can. J. Zool.* **71,** 515–523 (1993).
9. Johnson, L. S. & Taylor, E. B. The distribution of divergent mitochondrial DNA lineages of threespine stickleback (*Gasterosteus aculeatus*) in the northeastern Pacific Basin: post-glacial dispersal and lake accessibility. *J. Biogeogr.* **31,** 1073–1083 (2004).
10. Caldera, E. J. & Bolnick, D. I. Effects of colonization history and landscape structure on genetic variation within and among threespine stickleback (*Gasterosteus aculeatus*) populations in a single watershed. *Evol. Ecol. Res.* **10,** 575–598 (2008).
11. Deagle, B. E. *et al.* Population genomics of parallel phenotypic evolution in stickleback across stream–lake ecological transitions. *Proc. Biol. Sci.* **279,** 1277–1286 (2012).

12. Deagle, B. E., Jones, F. C., Absher, D. M., Kingsley, D. M. & Reimchen, T. E. Phylogeography and adaptation genetics of stickleback from the Haida Gwaii archipelago revealed using genome-wide single nucleotide polymorphism genotyping. *Mol. Ecol.* **22,** 1917–1932 (2013).

13. Kaeuffer, R., Peichel, C. L., Bolnick, D. I. & Hendry, A. P. Parallel and nonparallel aspects of ecological, phenotypic, and genetic divergence across replicate population pairs of lake and stream stickleback. *Evolution* **66,** 402–218 (2012).

14. Berner, D., Adams, D. C., Grandchamp, A.-C. & Hendry, A. P. Natural selection drives patterns of lake–stream divergence in stickleback foraging morphology. *J. Evol. Biol.* **21,** 1653–1665 (2008).

15. Mahler, D. L., Ingram, T., Revell, L. J. & Losos, J. B. Exceptional convergence on the macroevolutionary landscape in island lizard radiations. *Science* **341,** 292–295 (2013).

16. Marchinko, K. B., Matthews, B., Arnegard, M. E., Rogers, S. M. & Schluter, D. Maintenance of a genetic polymorphism with disruptive natural selection in stickleback. *Curr. Biol.* **24,** 1289–1292 (2014).

17. Kitano, J. *et al.* Reverse evolution of armor plates in the threespine stickleback. *Curr. Biol.* **18,** 769–774 (2008).

18. Bańbura, J. Lateral plate morph differentiation of freshwater and marine populations of the three-spined stickleback, *Gasterosteus aculeatus*, in Poland. *J. Fish Biol.* **44,** 773–783 (1994).

19. Leinonen, T., McCairns, R. J. S., Herczeg, G. & Merilä, J. Multiple evolutionary pathways to decreased lateral plate coverage in freshwater threespine sticklebacks. *Evolution* **66,** 3866–3875 (2012).

20. Gould, S. J. *Wonderful Life: The Burgess Shale and the Nature of History* (W. W. Norton & Co., 1989).

21. Nosil, P. & Crespi, B. J. Does gene flow constrain adaptive divergence or vice versa? A test using ecomorphology and sexual isolation in *Timema cristinae* walking-sticks. *Evolution* **58,** 102–112 (2004).

22. Kolbe, J. J., Leal, M., Schoener, T. W., Spiller, D. A. & Losos, J. B. Founder effects persist despite adaptive differentiation: a field experiment with lizards. *Science* **335,** 1086–1089 (2012).

23. Lucek, K., Lemoine, M. & Seehausen, O. Contemporary ecotypic divergence during a recent range expansion was facilitated by adaptive introgression. *J. Evol. Biol.* **27,** 2233–2248 (2014).

24. Theis, A., Ronco, F., Indermaur, A., Salzburger, W. & Egger, B. Adaptive divergence between lake and stream populations of an East African cichlid fish. *Mol. Ecol.* **23,** 5304–5322 (2014).

25. Berner, D., Grandchamp, A.-C. & Hendry, A. P. Variable progress toward ecological speciation in parapatry: stickleback across eight lake-stream transitions. *Evolution* **63,** 1740–1753 (2009).

26. Hanifin, C. T., Brodie, E. D. & Brodie, E. D. Phenotypic mismatches reveal escape from arms-race coevolution. *PLoS Biol.* **6,** e60 (2008).

27. Heinen, J. L. *et al.* Environmental drivers of demographics, habitat use, and behavior during a post-Pleistocene radiation of Bahamas mosquitofish (*Gambusia hubbsi*). *Evol. Ecol.* **27,** 971–991 (2013).

28. Ravinet, M., Prodöhl, P. A. & Harrod, C. Parallel and nonparallel ecological, morphological and genetic divergence in lake-stream stickleback from a single catchment. *J. Evol. Biol.* **26,** 186–204 (2013).

29. Adams, D. C. & Collyer, M. L. A general framework for the analysis of phenotypic trajectories in evolutionary studies. *Evolution* **63,** 1143–1154 (2009).

30. Hendry, A. P. & Taylor, E. B. How much of the variation in adaptive divergence can be explained by gene flow? An evaluation using lake-stream stickleback pairs. *Evolution* **58,** 2319–2331 (2004).

31. Peterson, B. K., Weber, J. N., Kay, E. H., Fisher, H. S. & Hoekstra, H. E. Double digest RADseq: an inexpensive method for *de novo* SNP discovery and genotyping in model and non-model species. *PLoS ONE* **7,** e37135 (2012).

32. Oke, K. B. *et al.* Does plasticity enhance or dampen phenotypic parallelism? A test with three lake-stream stickleback pairs. *J. Evol. Biol.* **29,** 126–143 (2015).

33. Zelditch, M. L., Swiderski, D. L & Sheets, H. D. *Geometric Morphometrics for Biologists: A Primer* (Elsevier, 2012).

34. Adams, D. C. & Otárola-Castillo, E. Geomorph: an rpackage for the collection and analysis of geometric morphometric shape data. *Methods Ecol. Evol.* **4,** 393–399 (2013).

35. Albert, A. Y. K. *et al.* The genetics of adaptive shape shift in stickleback: pleiotropy and effect size. *Evolution* **62,** 76–85 (2008).

36. Schindelin, J. *et al.* Fiji: an open-source platform for biological-image analysis. *Nat. Methods* **9,** 676–682 (2012).

37. Snowberg, L. K., Hendrix, K. M. & Bolnick, D. I. Covarying variances: more morphologically variable populations also exhibit more diet variation. *Oecologia* **178,** 89–101 (2015).

38. Rohland, N. & Reich, D. Cost-effective, high-throughput DNA sequencing libraries for multiplexed target capture. *Genome Res.* **22,** 939–946 (2012).

39. Catchen, J., Hohenlohe, P. A., Bassham, S., Amores, A. & Cresko, W. A. Stacks: an analysis tool set for population genomics. *Mol. Ecol.* **22,** 3124–3140 (2013).

40. Li, H. & Durbin, R. Fast and accurate short read alignment with Burrows-Wheeler transform. *Bioinformatics* **25,** 1754–1760 (2009).

41. Lunter, G. & Goodson, M. Stampy: a statistical algorithm for sensitive and fast mapping of Illumina sequence reads. *Genome Res.* **21,** 936–939 (2011).

42. Li, H. *et al.* The sequence alignment/map format and SAMtools. *Bioinformatics* **25,** 2078–2079 (2009).

43. Lleonart, J., Salat, J. & Torres, G. J. Removing allometric effects of body size in morphological analysis. *J. Theor. Biol.* **205,** 85–93 (2000).

Acknowledgements

Author contributions

A.P.H., C.L.P., R.D.H.B., D.H., B.K.L., Y.E.S. and D.I.B. planned the study. All authors executed the study. Y.E.S. oversaw field collections, conducted with D.I.B., C.L.P., A.P.H., R.D.H.B., D.H., B.K.L., T.T., A.D. and R.I. Y.E.S. oversaw morphological and environmental data collections by Y.E.S., D.I.B., C.J.T., T.T., N.A. and R.I. Y.E.S. collected genomic data with help from J.N.W. and D.I.B. Y.E.S., T.V. and D.I.B. analysed the data. M.R. estimated the population genetic parameters. All authors participated in the writing of the manuscript.

Additional information

Supplementary information is available for this paper.

Reprints and permissions information is available at www.nature.com/reprints.

Correspondence and requests for materials should be addressed to Y.E.S.

How to cite this article: Stuart, Y. E. *et al.* Contrasting effects of environment and genetics generate a continuum of parallel evolution. *Nat. Ecol. Evol.* **1,** 0158 (2017).

Publisher's note: Springer Nature remains neutral with regard to jurisdictional claims in published maps and institutional affiliations.

Competing interests

The authors declare no competing financial interests.